Authors' accepted manuscript.
Article accepted for publication in the IEEE International Conference on Robotics and Automation in Yokohama, Japan from May 13-17, 2024.
Version of record will be available at: https://ieeexplore.ieee.org/

Singularity Analysis of Kinova's Link 6 Robot Arm via Grassmann Line Geometry

Milad Asgari[1], Ilian A. Bonev[1], Clément Gosselin[2]
[1]*École de technologie supérieure (ÉTS)*, Montréal, QC, Canada
ilian.bonev@etsmtl.ca
[2]*Université Laval*, Québec, QC, Canada

***Abstract*—Unlike parallel robots, for which hundreds of different architectures have been proposed, the vast majority of six-degree-of-freedom (DOF) serial robots have one of two simple architectures. In both architectures, the inverse kinematics can be solved in closed form and the singularities described by trivial geometric and algebraic conditions. These conditions can be readily obtained by analyzing the determinant of the robot's Jacobian matrix, and provide an in-depth understanding of the robot's singularities, which is essential for its optimal use. However, for various reasons, robot arms with unorthodox architectures are occasionally designed. Such arms do not have closed-form inverse kinematics and little insight into their singularities can be gained by analyzing the determinant of their Jacobian. One such robot arm for which the conventional singularity analysis approach fails is the new Link 6 collaborative robot by Kinova. In this paper, we study the complex singularities of Link 6 by investigating all possibilities for screw dependencies, deriving a simple equation for each case, and then describing each singularity type using Grassmann line geometry. Twelve different singularity configurations are identified and described with seven relatively simple geometric conditions. Our approach is general and can be applied to other robot arms.**

***Index Terms*—Singularities, industrial robot arms, Screw dependency, Grassmann line geometry, Kinova Link 6.**

I. Introduction

Singularities are present in most mechanisms, defined as configurations where the velocity kinematics is indeterminate [1]. In a parallel robot, some singularities can be dangerous and lead to a mechanical failure [2]. There have been hundreds of parallel robot designs proposed and the study of their singularities has revealed various types of complex phenomena (e.g., [3], [4]). However, commercial parallel robots such as Fanuc's F-200iB hexapod, the various Delta robots, or SmarAct's positioning devices are designed in such a way that singularities cannot occur for the design parameters chosen (e.g., joint limits). Thus, in practice, even the most complex, commercial parallel robot is relatively simple to use.

In contrast, all six-degree-of-freedom (DOF) robot arms have singularities. Limiting the ranges of some of the robot arm's joints would prevent singularities from occurring, but would also significantly reduce the robot's workspace. Thus, in practice, all six-DOF robot arms have singularities. Singularities in robot arms are not dangerous, but they are a nuisance—an invisible barrier that must be constantly circumvented. Not understanding the singularities of a robot arm prevents a user from exploiting the robot's full potential.

Fortunately, about two-thirds of the few million industrial robots in operation are so-called articulated robots [5]. The vast majority of these robot arms have the same architecture as the PUMA robot developed in the 1970s by Victor Scheinman. Namely, they have six revolute joints, the axis of the first joint being vertical, the axes of the second and third joints being horizontal, and the axes of the last three joints intersecting at one point. The singularities of the PUMA-type architecture are well known and can be easily obtained by factoring the determinant of the Jacobian matrix of the robot [6].

The other popular six-DOF robot arm design is the one used by most collaborative robots, such as those from Universal Robots. The inverse kinematics and the singularities for this design are slightly different from those of the PUMA but are still trivial [7]. Indeed, Pieper [8] showed that robot arms with six revolute joints that have three joints with concurrent or parallel axes have closed-form inverse kinematics, which indirectly means singularities that are easy to describe.

Because of design considerations, such as improving dexterity, some robot manufacturers occasionally propose six-DOF robot designs that do not meet Pieper's criterion. Modern examples of such robots are most painting robots and Fanuc's CRX and Kinova's Link 6 collaborative robots. Little research has been dedicated to the analyses of the inverse kinematics and singularities of such unorthodox designs [9]–[12].

In a *kinematic singularity*, the end-effector of a 6-DOF robot arm loses at least one DOF, and its 6×6 Jacobian matrix, $\mathbf{J}$, becomes rank-deficient [13]. Thus, kinematic singularities in 6-DOF robot arms occur when $\det(\mathbf{J}) = 0$, which represents a trigonometric equation that is a function of the robot joint angles (all but the first and last one). For robot arms that do not respect Pieper's criterion, that equation is complex and cannot be factored into smaller expressions. Having such an equation, even if it were relatively small, is of very little use. Another method for gaining insight into the singularities of a robot arm is by studying the special cases of the inverse kinematics of

This work was funded by the Fonds de Recherche du Québec, Nature et Technologie (FRQNT)

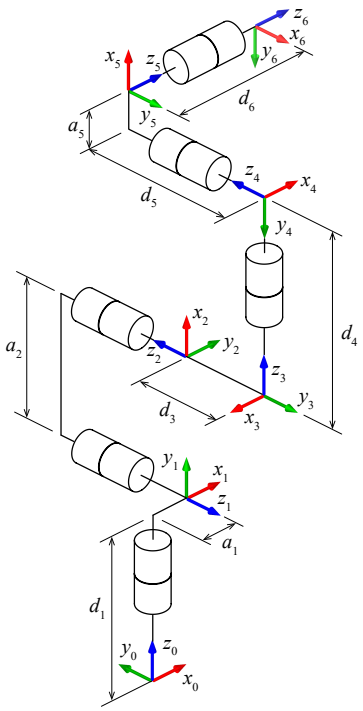

Fig. 1: The schematic of Kinova's Link 6 robot arm with its DH parameters and reference frames (all θ_i's are zero).

the robot. Unfortunately, these special cases cannot be studied when the inverse kinematics cannot be solved analytically.

In this paper, we study the singularities of Kinova's Link 6 6-DOF robot arm. Strictly speaking, in this robot, the only deviation from the PUMA's design is in the relative location of its sixth joint. The axis of that joint is offset in two directions: it does not intersect the axes of joints 4 and 5 (Fig. 1). We will show how these two offsets lead to multiple complex singularities. Yet, the methodology that we will employ will provide geometric insights into all of these singularities.

Instead of analyzing $\det(\mathbf{J})$, we will use the screw dependency approach [14]. In other words, we will categorize the robot's singularities by the sets of columns of the Jacobian matrix that are linearly dependent on a single rank deficiency. We will provide simple analytic expressions for each such category. Then, we will use Grassmann line geometry to describe the geometric conditions that constrain the corresponding joint axes [15], [16]. To the best of our knowledge, Grassmann geometry has only been used for parallel robots so far.

The remainder of this paper is organized as follows. In Section II, the direct kinematic model of Kinova's Link 6 is presented, and its Jacobian matrix is derived. In Section III, the kinematic singularities of the robot are categorized into different families in terms of their geometric conditions. Finally, Section IV concludes the paper.

II. Robot's Direct Kinematics and Jacobian Matrix

Kinova's Link 6 is a 6-DOF collaborative robot arm with revolute joints, in which the axes ($\mathcal{L}_i$) of its joints are constrained as follows: $\mathcal{L}_1 \perp \mathcal{L}_2 \parallel \mathcal{L}_3 \perp \mathcal{L}_4 \perp \mathcal{L}_5 \perp \mathcal{L}_6$.

TABLE I: DH parameters of Kinova's Link 6 robot arm.

i	θ_i	d_i	a_i	α_i
1	$-\theta_1$	190.500 mm	110.240 mm	90°
2	$\theta_2 + 90°$	0	485 mm	180°
3	$\theta_3 + 90°$	−22.447 mm	0	−90°
4	$\theta_4 - 180°$	−374.910 mm	0	90°
5	$\theta_5 + 90°$	−139.879 mm	−86 mm	90°
6	$\theta_6 + 90°$	179.028 mm	0	180°

As already mentioned, the only difference with the PUMA design is that $\mathcal{L}_6$ does not intersect $\mathcal{L}_5$ and $\mathcal{L}_4$. Figure 1 shows a schematic of the arm with its principal dimensions.

The (conventional) Denavit and Hartenberg (DH) parameters of the Link 6 are given in Table I [18]. These DH parameters can be used to transform two consecutive frames into each other as:

$$ {}^{i-1}_{i}\mathbf{T} = \mathbf{T}_{z_i}(d_i)\mathbf{R}_{z_i}(\theta_i)\mathbf{T}_{x_i}(a_i)\mathbf{R}_{x_i}(\alpha_i). \tag{1} $$

Equation (1) describes the position and orientation of frame $\mathrm{F_i}$ with respect to frame F_{i-1}, where $\mathbf{R}_{z_i}(\theta_i)$ represents a pure rotation about the z_i axis by θ_i, $\mathbf{T}_{z_i}(d_i)$ represents a pure translation along the z_i axis by d_i, $\mathbf{T}_{x_i}(a_i)$ represents a pure translation along the x_i axis by a_i, and $\mathbf{R}_{x_i}(\alpha_i)$ represents a pure rotation about the x_i axis by α_i.

Therefore, the relative pose of two consecutive link-frames can be expressed using this homogeneous transformation matrix as function of the joint angle (Figure 1). Then, the forward kinematic equation can be obtained by:

$$ {}^{0}_{6}\mathbf{T} = {}^{0}_{1}\mathbf{T}\,{}^{1}_{2}\mathbf{T}...{}^{5}_{6}\mathbf{T}, \tag{2} $$

where

$$ {}^{i-1}_{i}\mathbf{T} = \begin{bmatrix} C_{\theta_i} & -S_{\theta_i}C_{\alpha_i} & S_{\theta_i}S_{\alpha_i} & a_iC_{\theta_i} \\ S_{\theta_i} & C_{\theta_i}C_{\alpha_i} & -C_{\theta_i}S_{\alpha_i} & a_iS_{\theta_i} \\ 0 & S_{\alpha_i} & C_{\alpha_i} & d_i \\ 0 & 0 & 0 & 1 \end{bmatrix}, \tag{3} $$

and C_{θ_i}, S_{θ_i}, are respectively $\cos(\theta_i)$, $\sin(\theta_i)$, etc.

It has been shown that by choosing an appropriate reference frame to represent joint screws, the Jacobian matrix can be made simpler. The determinant of the Jacobian matrix is independent of this choice of frame. In complex manipulators, the Jacobian elements tend to be more compact when choosing the middle frame to express the joint screws [19]. Therefore, we set F_4 as the main reference frame and the i-th joint screw, ${}^4\$_i$, which represents the momentary motion of that joint is expressed in F_4:

$$ {}^4\$_i = \begin{bmatrix} \mathbf{e}_i \\ \mathbf{e}_i \times \mathbf{r}_i, \end{bmatrix}, \tag{4} $$

where $\mathbf{e}_i$ is the unit vector along joint axis i, and $\mathbf{r}_i$ is the vector between the origins of the i-th link frame and the base reference frame (frame 4), both vectors expressed with respect to frame 4. Thus, we have:

$$
{}^4\mathbf{J} = \begin{bmatrix} {}^4\$_1 & {}^4\$_2 & {}^4\$_3 & {}^4\$_4 & {}^4\$_5 & {}^4\$_6 \end{bmatrix} = \begin{bmatrix} S_{2,-3} & 0 & 0 & 0 & -S_4 & -C_4C_5 \\ 0 & 1 & -1 & 0 & C_4 & -S_4C_5 \\ -C_{2,-3} & 0 & 0 & 1 & 0 & S_5 \\ -d_3C_{2,-3} & -a_2C_3 & 0 & 0 & -d_4C_4 & d_5C_4S_5 + (d_4C_5 + a_5)S_4 \\ a_2S_2 - a_1 & 0 & 0 & 0 & -d_4S_4 & d_5S_4S_5 - (d_4C_5 + a_5)C_4 + d_5S_4S_5 \\ -d_3S_{2,-3} & a_2S_3 & 0 & 0 & 0 & d_5C_5 \end{bmatrix}, \quad (5)
$$

$$
\begin{aligned} |{}^4\mathbf{J}| = a_2 \Bigg(& d_4S_3C_5(d_5C_2S_4C_3 + a_1) + a_1S_3S_4(d_4C_4S_5 + a_5S_4) + C_5(a_1d_5C_3S_4 + d_4^2C_2S_3^2) - d_4a_5S_2C_2S_3^2 \\ & \Big(d_4S_3C_5(d_4C_3 + a_2) + a_5d_4S_3C_3 + a_2S_3S_4(d_5C_4S_5 + a_5S_4) + d_5C_3S_4C_5(d_4C_3 + a_2) + d_3S_4(a_5C_4 - d_5S_5S_4)\Big)\Bigg), \end{aligned} \quad (6)
$$

where $S_i = \sin\theta_i$, $C_i = \cos\theta_i$, $S_{i,-j} = \sin(\theta_i - \theta_j)$, $C_{i,-j} = \cos(\theta_i - \theta_j)$, $C_{i,j} = \cos(\theta_i + \theta_j)$.

III. Analyses of all Kinematic Singularities

Kinematic singularities arise when the Jacobian matrix becomes rank deficient, indicating a dependency among its six rows or columns. In essence, the rank deficiency equals the count of dependency among columns. Another method to identify these singular configurations is by analyzing the determinant of the Jacobian matrix when zeroed, as defined in equation (6). In other words, a singularity is a sufficient and necessary condition for the determinant to vanish. However, this equation is complex and impossible to exploit in the case of Kinova's Link 6. Furthermore, it does not elucidate which joint screws are mutually dependent in each singular case.

The determinant expressed in (6) is much more complex than the one for the PUMA robot [7] and the one for the UR5 robot [6] and cannot be factored. Consequently, in this paper, we propose a new approach for identifying kinematic singularities. We classify these singularities based on Grassmann line geometry into five different categories, providing a clearer understanding of the dependencies among screws in different kinematic singularities [15], [16]. The geometric conditions presented here (Table II and Fig. 2) correspond to kinematic singularities, as proven by screw theory, but they are also associated with simple symbolic expressions resulting from the analysis of dependencies in the Jacobian matrix's columns (i.e., the joint screws).

To uncover the relationships among various combinations of joint screws, we conducted a comprehensive analysis. First, we focused on pairs of screws, examining dependencies such as (${}^4\$_1$, ${}^4\$_2$), (${}^4\$_1$, ${}^4\$_3$), all the way to (${}^4\$_5$, ${}^4\$_6$). Next, we extended our analysis to three-screw dependencies, exploring combinations like (${}^4\$_1$, ${}^4\$_2$, ${}^4\$_3$), (${}^4\$_1$, ${}^4\$_2$, ${}^4\$_4$), and so on. Finally, we delved into four-screw and five-screw dependencies, considering sets like (${}^4\$_1$, ${}^4\$_2$, ${}^4\$_3$, ${}^4\$_4$), (${}^4\$_1$, ${}^4\$_2$, ${}^4\$_3$, ${}^4\$_4$, ${}^4\$_5$). To establish equations for these dependencies, we employed the principles of linear algebra, particularly the concept of dependent vectors. Here, we illustrate how we derived an equation for the dependency involving (${}^4\$_1$, ${}^4\$_6$), and for the others, we utilized the same approach.

To assess the dependency between these two screws, we arrange them into a 2×6 matrix. To determine their dependency, we repeatedly remove four distinct rows and compute the determinant of the resulting 2×2 matrix, resulting in 15 different equations, ${}^{6!}/_{2!\,(6-2)!}$, denoted as eq_1, eq_2, and so on up to eq_{15}. For these screws to be considered dependent, each of these 15 equations must yield a result of zero. Consequently, we calculate these equations and eliminate those that exhibit dependency or are already equal to zero.

In the end, since all of these expressions must be equal to zero, we formulate a final equation in the form of:

$$
eq_1^2 + eq_2^2 + ... + eq_n^2 = 0, \quad (7)
$$

for brevity (instead of proving n individual equations).

Category A: Two-screw dependency

The first category is when two joint axes become aligned [16]. As Table II shows, when this condition occurs, the end-effector loses one degree of freedom, causing the rank of the Jacobian matrix to drop to 5. Since there should be four specific joint angles in this singular configuration, it is possible to find a path in joint space between any two non-singular joint sets without crossing this type of singularity. We will loosely refer to such a singularity as an *avoidable singularity*. By defining $\mathcal{L}_i$ as the i-th joint axis, and employing the operator $\equiv$ to designate that two axes are collinear, here is the single possible case for category A:

A: $\mathcal{L}_1 \equiv \mathcal{L}_6$ (Fig. 2a).

This singular configuration occurs when axes 1 and 6 coincide and can be described by (8) after screw dependency analysis between ${}^4\$_1$ and ${}^4\$_6$:

$$
\begin{aligned} (-a_5S_4 - d_5C_4 + d_3)^2 + S_{2,-3}^2 + C_5^2 \\ +(a_5C_4 - d_5S_4 - a_2S_3 + a_1)^2 = 0. \end{aligned} \quad (8)
$$

This equation has only several solutions, one of which is shown in Table II and Fig. 2a.

TABLE II: Examples of joint positions for each type of kinematic singularity in Kinova's Link 6 robot arm.

Case	Condition	Examples of joint positions*
A	$\mathcal{L}_1 \equiv \mathcal{L}_6$, which can only happen when $\mathcal{L}_4 \| \mathcal{L}_1$	0°, 34.24°, 34.24°, 113.72°, 0°, 0° (Fig. 2a)
B_1	$\mathcal{L}_1$, $\mathcal{L}_4$, $\mathcal{L}_6$ ▨	0°, 60°, 60°, −125.72°, −90°, 0° (Fig. 2b)
B_2	$\mathcal{L}_2$, $\mathcal{L}_3$, $\mathcal{L}_6$ ▨	0°, 30°, 16.84°, 90°, 50°, 0°
B_3	$\mathcal{L}_2$, $\mathcal{L}_3$, $\mathcal{L}_5$ ▨	0°, 30°, 0°, 0°, 30°, 0°
C_1	$\mathcal{L}_1$, $\mathcal{L}_2$, $\mathcal{L}_3$, $\mathcal{L}_5$ belong to two planar pencils with a common line	0°, 13.14°, 13.14°, 0°, 30°, 0° (Fig. 2c)
C_2	$\mathcal{L}_1$, $\mathcal{L}_3$, $\mathcal{L}_4$, $\mathcal{L}_5$ ▨	−162.95°, 20°, 0°, −148.7°, 90°, 0° (Fig. 2d)
C_3	$\mathcal{L}_2$, $\mathcal{L}_3$, $\mathcal{L}_4$, $\mathcal{L}_6$ ▨	−250°, −33.07°, −123.06°, 92.23°, −20°, 0° (Fig. 2e)
D_1	$\mathcal{L}_1$, $\mathcal{L}_2$, $\mathcal{L}_3$, $\mathcal{L}_4$, $\mathcal{L}_5$ are concurrent with two lines	0°, 17.19°, 22.25°, 62.10°, 160°, 0° (Fig. 2f)
D_2	$\mathcal{L}_2$, $\mathcal{L}_3$, $\mathcal{L}_4$, $\mathcal{L}_5$, $\mathcal{L}_6$ are concurrent with two lines	0°, 60°, −16.66°, −99.22°, 5.73°, 0°
D_3	$\mathcal{L}_3$, $\mathcal{L}_4$, $\mathcal{L}_5$ in a plane, $\mathcal{L}_1 \| \mathcal{L}_6$ and parallel to that plane	0°, 60°, −120°, 0°, −90°, 0° (Fig. 2g)
D_4	$\mathcal{L}_1$ and $\mathcal{L}_6$ in a plane, $\mathcal{L}_2 \| \mathcal{L}_3 \| \mathcal{L}_5$ and parallel to that plane	0°, −20°, −95°, 0°, −165°, 0° (Fig. 2h)
E	$\mathcal{L}_1$, $\mathcal{L}_2$, $\mathcal{L}_3$, $\mathcal{L}_4$, $\mathcal{L}_5$, $\mathcal{L}_6$ are concurrent with one line	0°, −40°, −100°, 0°, −40.06°, 0° (Fig. 2i)

* Joint angles presented in gray can be arbitrary.

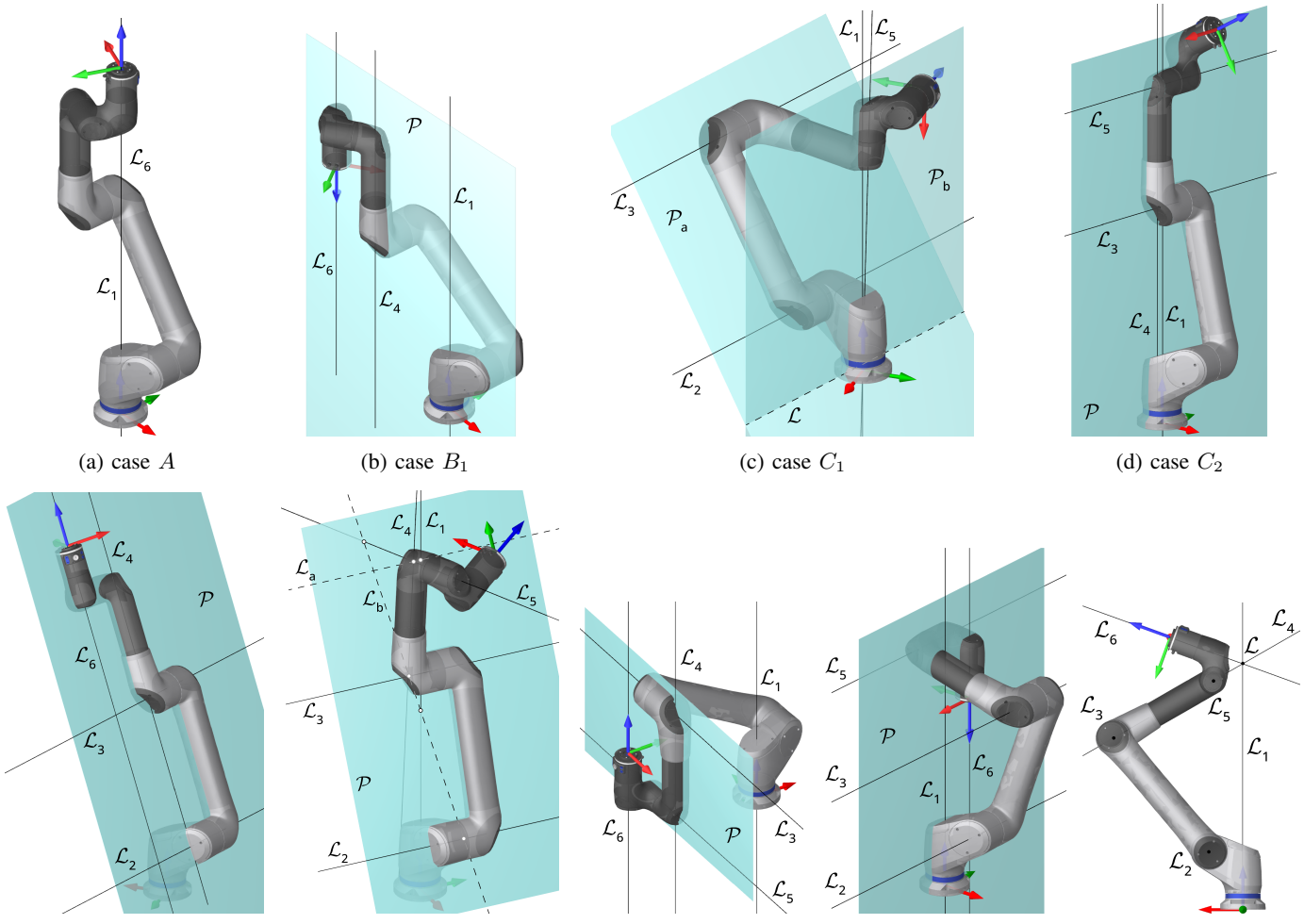

Fig. 2: Geometric interpretation of each type of kinematic singularity present in Kinova's Link 6 robot arm.

Category B: Three-screw dependency

In the second category, we have three joint axes that are parallel and coplanar [16]. Some combinations of joint screws do not meet this condition, such as when one of these three joints is the first joint of the manipulator and the other is the second joint of the manipulator since they are always perpendicular to each other. This category can be divided into three subcategories, as shown in Table II, after dependency analyses among various combinations. Again, the robot end-effector loses one DOF, and at least two different joint angles should be unique; therefore, these singularities too are avoidable.

B_1: $\mathcal{L}_1$, $\mathcal{L}_4$, and $\mathcal{L}_6$ are parallel and coplanar (Fig. 2b).
This singularity can be described by (9) after screw dependency analysis between ${}^4\$_1$, ${}^4\$_4$ and ${}^4\$_6$:

$$\Big((a_2d_5S_3 - a_1d_5 - a_5d_3)C_4 + a_2a_5S_3 - a_1a_5 + d_3d_5\Big)^2 + S^2_{2,^-3} + S^2_5 = 0. \tag{9}$$

This equation has only several solutions, one of which is shown in Table II and Fig. 2b. It can be shown that category A is actually a special case of B_1, because if $\mathcal{L}_1 \equiv \mathcal{L}_6$, then $\mathcal{L}_4$ must be parallel to them ($\theta_2 = \theta_3$).

B_2: $\mathcal{L}_2$, $\mathcal{L}_3$, and $\mathcal{L}_6$ are parallel and coplanar.
This singularity can be described by (10) after screw dependency analysis between ${}^4\$_2$, ${}^4\$_3$ and ${}^4\$_6$:

$$\Big((a_5 + d_4)S_3 + d_5C_3\Big)^2 + C^2_4 + S^2_5 = 0. \tag{10}$$

This equation too has only several solutions, one of which is shown in Table II. (We do not provide a figure for this subcategory, since it is very similar to B_1.)

B_3: $\mathcal{L}_2$, $\mathcal{L}_3$, and $\mathcal{L}_5$ are parallel and coplanar.
This singularity can be described by (11) after screw dependency analysis between ${}^4\$_2$, ${}^4\$_3$ and ${}^4\$_5$:

$$S^2_3 + S^2_4 = 0. \tag{11}$$

This equation too has only several solutions, one of which is shown in Table II. (We do not provide a figure for this subcategory, since it is very similar to B_1.)

Category C: Four-screw dependency

In the third category, a set of four joint axes are coplanar or belong to the union of two planar pencils that have a line in common [16]. This category can be divided into three subcategories. Again, the robot end-effector loses one DOF, and at least three angles should be unique; therefore, these singularities too are avoidable.

C_1: $\mathcal{L}_1$, $\mathcal{L}_5$ and a line $\mathcal{L}$ are coplanar and concurrent, and $\mathcal{L}$ is parallel to and coplanar with $\mathcal{L}_2$ and $\mathcal{L}_3$ (Fig. 2c).
This singularity can be described by (12) after screw dependency analysis between ${}^4\$_1$, ${}^4\$_2$, ${}^4\$_3$ and ${}^4\$_5$:

$$(a_2C_3 - a_1 - d_4)^2 + C^2_{2,^-3} + (d_3S_4C_3 + d_4S_3C_4)^2 = 0. \tag{12}$$

This equation has only several solutions, one of which is shown in Table II and Fig. 2c.

C_2: $\mathcal{L}_1$, $\mathcal{L}_3$, $\mathcal{L}_4$, and $\mathcal{L}_5$ are coplanar (Fig. 2d).
This singularity can be described by (13) after screw dependency analysis between ${}^4\$_1$, ${}^4\$_3$, ${}^4\$_4$ and ${}^4\$_5$:

$$(d_5S_4 - a_5C_4)^2 + C^2_5 + S^2_3 = 0. \tag{13}$$

This equation too has only several solutions, one of which is shown in Table II and Fig. 2c. In all solutions, $\mathcal{L}_1||\mathcal{L}_4$ and $\mathcal{L}_3||\mathcal{L}_5$.

C_3: $\mathcal{L}_2$, $\mathcal{L}_3$, $\mathcal{L}_4$, and $\mathcal{L}_6$ are coplanar (Fig. 2e).
This singularity can be described by (14) after screw dependency analysis between ${}^4\$_2$, ${}^4\$_3$, ${}^4\$_4$ and ${}^4\$_6$:

$$(a_1 - a_2S_3)^2 + S^2_{2,^-3} + S^2_4 = 0. \tag{14}$$

This equation too has only several solutions, one of which is shown in Table II and Fig. 2e. In all solutions, $\mathcal{L}_4||\mathcal{L}_6$.

Category D: Five-screw dependency

In the fourth category, we either have five joint axes concurrent with two lines, or three of them in one plane and the other two parallel to each other and to the plane [16]. The robot end-effector loses one DOF, and at least three joint angles should be unique. Therefore, these singularities too are avoidable.

D_1: $\mathcal{L}_1$, $\mathcal{L}_2$, $\mathcal{L}_3$, $\mathcal{L}_4$, and $\mathcal{L}_5$ all intersect two lines, $\mathcal{L}_a$ and $\mathcal{L}_b$ (Fig. 2f).
This singularity can be described by (15) after screw dependency analysis between ${}^4\$_1$, ${}^4\$_2$, ${}^4\$_3$, ${}^4\$_4$ and ${}^4\$_5$:

$$\Big((d_5S_4C_4S_5 + a_5S^2_5 + d_4C_5)S_3 + d_5S_4C_3C_5\Big)^2 + \Big((d_4C_5 + a_5)S_3 + d_5C_3C_5S_4\Big)^2 + C^2_3(d_5S_4S_5 - a_5C_4)^2 = 0. \tag{15}$$

This equation has infinitely many solutions. In all solutions, one of which is shown in Table II and Fig. 2f, line $\mathcal{L}_a$ is parallel to and coplanar with axes $\mathcal{L}_2$ and $\mathcal{L}_3$, and line $\mathcal{L}_b$ is in the same plane as these three lines.

D_2: $\mathcal{L}_2$, $\mathcal{L}_3$, $\mathcal{L}_4$, $\mathcal{L}_5$, and $\mathcal{L}_6$ all intersect two lines.
This singularity can be described by (16) after screw dependency analysis between ${}^4\$_2$, ${}^4\$_3$, ${}^4\$_4$, ${}^4\$_5$ and ${}^4\$_6$:

$$C^2_{2,5,^-3} + S^2_4 + \Big(a_5S_{2,^-3} + C_5(a_1 - a_2S_2 + d_4S_{2,^-3})\Big)^2 + \Big(S_5(a_1 - a_2S_2) + C_{2,3}(a_5 + d_4C_5)\Big)^2 = 0, \tag{16}$$

where $C_{2,5,-3} = \cos(\theta_2 + \theta_5 - \theta_3)$. This equation too has infinitely many solutions, one of which is shown in Table II. (We do not provide a figure for this subcategory, since it is very similar to D_1.)

D_3: $\mathcal{L}_3$, $\mathcal{L}_4$, $\mathcal{L}_5$ lie in one plane, and $\mathcal{L}_1$ and $\mathcal{L}_6$ are parallel to each other and to that plane (Fig. 2g).

This singularity can be described by (17) after screw dependency analysis between ${}^4\$_1$, ${}^4\$_3$, ${}^4\$_4$, ${}^4\$_5$ and ${}^4\$_6$:

$$S_{2,^-3}^2 + S_4^2 + C_5^2 = 0. \tag{17}$$

This equation has infinitely many solutions, one of which is shown in Table II and Fig. 2g. In all solutions, $\mathcal{L}_1||\mathcal{L}_4||\mathcal{L}_6$ and $\mathcal{L}_3||\mathcal{L}_5$.

D_4: $\mathcal{L}_1$, $\mathcal{L}_3$, $\mathcal{L}_6$ lie in one plane, and $\mathcal{L}_2$ and $\mathcal{L}_5$ are parallel to each other and to that plane (Fig. 2h).
This singularity can be described by (18) after screw dependency analysis between ${}^4\$_1$, ${}^4\$_2$, ${}^4\$_3$, ${}^4\$_5$ and ${}^4\$_6$:

$$\begin{aligned}\Big(S_3C_4(a_1 - a_2S_2) - d_2S_2S_4\Big)^2 \\ +(a_1 - a_2S_2 + d_4S_{2,^-3})^2 \\ -\Big(d_3C_4(C_3S_{2,3} + C_2) + d_2S_2S_4\Big)^2 = 0.\end{aligned} \tag{18}$$

This equation too has infinitely many solutions, one of which is shown in Table II and Fig. 2h. In all solutions, $\mathcal{L}_1||\mathcal{L}_6$ and $\mathcal{L}_2||\mathcal{L}_3||\mathcal{L}_5$.

Category E: Six-screw dependency

In the last, fifth category, all six joint axes must be concurrent with one line [16]. Since $\mathcal{L}_2||\mathcal{L}_3$, it can be shown than $\mathcal{L}_5$ must be parallel to these two lines too, i.e., $S_4 = 0$. Thus, we only have one subcategory.

E: $\mathcal{L}_2||\mathcal{L}_3||\mathcal{L}_5$ and $\mathcal{L}_1$, $\mathcal{L}_4$ and $\mathcal{L}_6$ intersect a line $\mathcal{L}$ that is parallel to the three other axes (Fig. 2i).
From the condition $S_4 = 0$, (6) reduces to

$$a_2d_4S_3\Big((a_1 - a_2S_2 + d_4S_{2,^-3})C_5 + a_5S_{2,^-3}\Big) = 0. \tag{19}$$

Eliminating the solution $S_3 = 0$, which would also lead to a subcategory B_3 singularity, for every θ_2 and θ_3, for which $a_1 - a_2S_2 + d_4S_{2,^-3} \neq 0$, we can find two solutions for θ_5 (actually four, because all robot's joints can rotate $\pm 360°$). The robot end-effector loses one DOF, and four joint angles should be unique. Therefore, these singularities too are avoidable.

Of course, some of the categories that we listed are special cases of other subcategories. However, we prefer to list them separately, as they may have particularities. For example, category A is a special case of category B_1, but in A, we can have a passive motion: the robot arm may rotate about axis 1, without affecting the pose of the end-effector.

In all of these categories, there is only a single end-effector DOF lost and none of these conditions can be combined together to lead to a loss of two DOFs, except for conditions E_1 and B_3, as we just saw. We also demonstrated that all of the kinematic singularities require at least two specific joint angles. Therefore, the manipulator can move from one non-singular joint set to another one without passing through a kinematic singularity. We can thus presume that the robot is *cuspidal*, as already mentioned in [20].

A cuspidal robot can move from one solution of the inverse kinematics for a given pose to another solution, without passing through a kinematic singularity. In a cuspidal robot, extreme care must be taken into finding ways to unequivocally describe a robot configuration [21]. For example, in a typical PUMA-type robot, we usually describe a configuration (i.e., the parameters that can be used to pinpoint a specific solution of the inverse kinematics) using the three binary parameters front/back, elbow-up/elbow-down, and flip/no-flip, in addition to prescribing the turn number for joints that can rotate more than $360°$. Failure to find a similar configuration description method may lead to a situation where the cuspidal robot repeats a sequence of Cartesian movements (so-called point-to-point movements, where a desired pose is given as the final destination) and ends up in a completely different joint position. Such unpredictable behavior is not only hazardous but can also result in production halts due to joint limits.

IV. Conclusion and Further Work

In conclusion, our research has demonstrated that the kinematic singularities exhibited by Kinova's Link 6 robot arm are distinct from the well-known wrist, elbow, and shoulder singularities commonly observed in standard 6-DOF PUMA-type robots. Moreover, we have illustrated that Kinova's Link 6 robot has a wide variety of singularities. We have provided clear geometric conditions for each kinematic singularity, offering a precise insight into the robot's kinematic behavior. These singularities can be categorized based on unique geometric conditions, which include five different categories: collinear joint axes, parallelism of three joint axes within the same plane, coplanarity of four joint axes, concurrence with two lines of five joint axes, coplanarity of three joint axes and parallelism with two other, and concurrence of all six joint axes with another line.

Our use of the "screw dependency" perspective has unveiled a more intuitive approach for analyzing singularities compared to traditional Jacobian determinant-based methods and eliminates the need to delve into complex determinant-based expressions by providing simpler equations for each category. In fact, in the case of Kinova's Link 6 robot arm, the traditional approach to analysing singularities fails. In addition, we used Grassmann line geometry, for the first time in a serial robot, to explain the geometric relationships between the joint axes corresponding to the dependent joint screws.

This paper opens up new possibilities for manufacturers to design and optimize new manipulators, while also providing automated production engineers with intuitive insights for programming robot arms to avoid singularities. In our future endeavors, we plan to apply the same methodology to explore the singularities of two 7-DOF robot arm designs with multiple non-zero joint offsets: ABB's YuMi and Kassow Robots' KR series. However, for a seven-joint robot arm, our approach necessitates exploring a significantly larger number of combinations of joint screw dependencies.

REFERENCES

[1] K.H. Hunt, *Kinematic geometry of mechanisms*, Clarendon press, Oxford, 1978.

[2] J.-P. Merlet, *Parallel Robots*, Springer, 2005.

[3] D. Zlatanov, I.A. Bonev, and C. Gosselin, "Constraint singularities of parallel mechanisms," *2002 IEEE International Conference on Robotics and Automation (ICRA)*, pp. 496–502, 2002.

[4] M. Conconi and M. Carricato, "A new assessment of singularities of parallel kinematic chains," *IEEE Transactions on Robotics*, vol. 25, no. 4, pp. 757–770, 2009.

[5] International Federation of Robotics, World of Robotics, 2022.

[6] M.J.D. Hayes, M.L. Husty, and P.J. Zsombor-Murray, "Singular configurations of wrist-partitioned 6R serial robots: a geometric perspective for users," *Transactions of the Canadian Society for Mechanical Engineering*, vol. 26, no. 1, pp. 41–55, 2002.

[7] M. FarzanehKaloorazi and I.A. Bonev, "Singularities of the typical collaborative robot arm," *2018 ASME International Design Engineering Technical Conferences and Computers and Information in Engineering Conference*, Quebec City, Quebec, Canada, 2018.

[8] D. Pieper, *The kinematics of manipulators under computer control*, Stanford University, 1969.

[9] X. Wang, D. Zhang, C. Zhao, H. Zhang, and H. Yan, "Singularity analysis and treatment for a 7R 6-DOF painting robot with non-spherical wrist," *Mechanism and Machine Theory*, vol. 126, pp. 92–107, 2018.

[10] S. Kucuk and Z. Bingul, "Inverse kinematics solutions for industrial robot manipulators with offset wrists," *Applied Mathematical Modelling*, vol. 38, no. 7–8, pp. 1983–1999, 2014.

[11] C. Gosselin and H. Liu, "Polynomial inverse kinematic solution of the Jaco robot," *ASME 2014 International Design Engineering Technical Conferences and Computers and Information in Engineering Conference*, Vol. 46377, paper No. DETC2014-34152, Buffalo, New-York, USA, 2014.

[12] G. Gogu, "Families of 6R orthogonal robotic manipulators with only isolated and pseudo-isolated singularities," *Mechanism and Machine Theory*, vol. 37, pp. 1347–1375, 2002.

[13] K. Hunt, "Robot kinematics—A compact analytic inverse solution for velocities," *Journal of Mechanisms, Transmissions, and Automation in Design*, vol. 109, no. 3, pp. 42–49, 1987.

[14] X. Kong and C. Gosselin, "A dependent-screw suppression approach to the singularity analysis of a 7-DOF redundant manipulator: CANADARM2," *Transactions of the Canadian Society for Mechanical Engineering*, vol. 29, pp. 593–604, 2005.

[15] J.-P. Merlet, "Singular configurations of parallel manipulators and Grassmann geometry," *International Journal of Robotics Research*, vol. 85, no. 5, pp. 45–56, 1989.

[16] F. Hao and J.M. McCarthy, "Conditions for line-based singularities in spatial platform manipulators," *Journal of Robotic Systems*, vol. 15, no. 1, pp. 43–55, 1998.

[17] G. Chen, L. Zhang, Q. Jia, and H. Sun, "Singularity analysis of redundant space robot with the structure of Canadarm2," *Mathematical Problems in Engineering*, vol. 2014, pp. 1–9, 2014.

[18] J. Denavit and R. Hartenberg, "A kinematic notation for lower-pair mechanisms based on matrices," *Journal of Applied Mechanics*, vol. 22, no. 2, pp. 215–221, 1995.

[19] K. Waldron, S. Wang, and S. Bolin, "A study of the Jacobian matrix of serial manipulators," *Journal of Mechanisms, Transmissions, and Automation in Design*, vol. 107, no. 6, pp. 230–237, 1985.

[20] P. Wenger and D. Chablat, "A review of cuspidal serial and parallel manipulators," *Journal of Mechanisms and Robotics*, vol. 15, no. 4, 2023.

[21] D. H. Salunkhe, D. Chablat, and P. Wenger, "Trajectory planning issues in cuspidal commercial robots," *2023 IEEE International Conference on Robotics and Automation (ICRA)*, London, United Kingdom, 2023.